Generation of a general Cowden clay model (GCCM) using a data-driven method

I. Kamas, H.J. Burd, B.W. Byrne
Department of Engineering Science, University of Oxford, England

S. K. Suryasentana
Civil and Environmental Engineering, University of Strathclyde, Glasgow

ABSTRACT: Monopiles are the most widespread foundation option for offshore wind turbines. The PISA (Pile Soil Analysis) joint industry research established a one-dimensional (1D) model for calculating the monotonic behaviour of laterally loaded monopiles by using a parametric equation to represent the soil reaction components. During the current PICASO project, a new data-driven method has been developed, as an alternative form of the PISA design model, in which Gaussian process regression (GPR) is employed to formulate the soil reaction curve data that are required to drive the 1D model to predict the monopile's monotonic behaviour. This paper presents a general Cowden clay model (GCCM) generated by using this data-driven method. The 1D model employing the GCCM can be used to predict the initial stiffness and ultimate capacity of piles embedded in homogenous glacial clay till soils within a range of different stress histories.

1 **Introduction**

Offshore wind turbine support structures are typically supported by monopile foundations. Monopiles are large diameter circular hollow steel tubes with a wall thickness that usually varies along the length of the pile. The design of monopiles requires analysis tools that can provide reliable and rapid predictions of the foundation capacity for environmental loads due to wind, waves and current. Design analyses are also required to determine the stiffness of the foundation, to facilitate estimates of the natural frequency of the overall structure.

Generalised models allow monopile design calculations to be conducted for a range of soil strength and stiffness profiles. An example of such a model is the PISA 1D general Dunkirk sand model (GDSM) (Burd et al., 2020), which is appropriate for sand within a range of relative densities. The current paper describes a new generalised model for glacial clay till, for incorporation in the PISA one-dimensional (1D) analysis framework. The model is referred to as 'general Cowden clay model' (GCCM); the reference to 'Cowden' signifies that the soil characteristics adopted in the model are based on the Cowden test site employed in the PISA project (Zdravkovic et al., 2020a, b). The GCCM employs a data-driven method that has been developed during the current PICASO project at Oxford University; the model is capable of predicting the monotonic loading response of a pile embedded in a homogenous glacial clay till soil with a range of potential stress history scenarios.

1.1 *Conventional design practice*

Conventional design procedures e.g. DNV-GL (2016) employ a simplified 1D analysis design model known as the *p-y* method. In the *p-y* method the pile is modelled as an embedded beam and the lateral soil response is represented by *p-y* curves, which are non-linear relationships between the distributed lateral load acting on the pile and the local lateral pile displacement. This method was developed for relatively slender piles; it is considered unreliable for offshore monopiles which employ a relatively small pile slenderness ratio, *L/D* (e.g. Byrne et al., 2017).

1.2 *The PISA design model*

The PISA (Pile Soil Analysis) project established the 'PISA design model' for monotonic analysis of laterally loaded monopiles (Byrne et al., 2020b; Burd et al., 2020). The model is able to conduct rapid calculations to determine the pile displacements and the distribution of bending moment and shear force acting in the pile. The PISA design model incorporates four soil reaction components; it provides an effective means of predicting the response of low length-to-diameter (L/D) relatively rigid piles within a pre-defined calibration space. The PISA soil reaction components (Figure 1(a)) acting on the pile are: (a) distributed lateral load; (b) distributed moment due to vertical shear tractions; (c) a horizontal force at the pile base; and (d) a moment at the pile base.

This is a peer-reviewed, accepted author manuscript of the following paper Kamas, I., Burd, H. J., Byrne, B. W., & Suryasentana, S. (2023). Generation of a general Cowden clay model (GCCM) using a data-driven method. Paper presented at Session on 'Pile Design', London, United Kingdom.

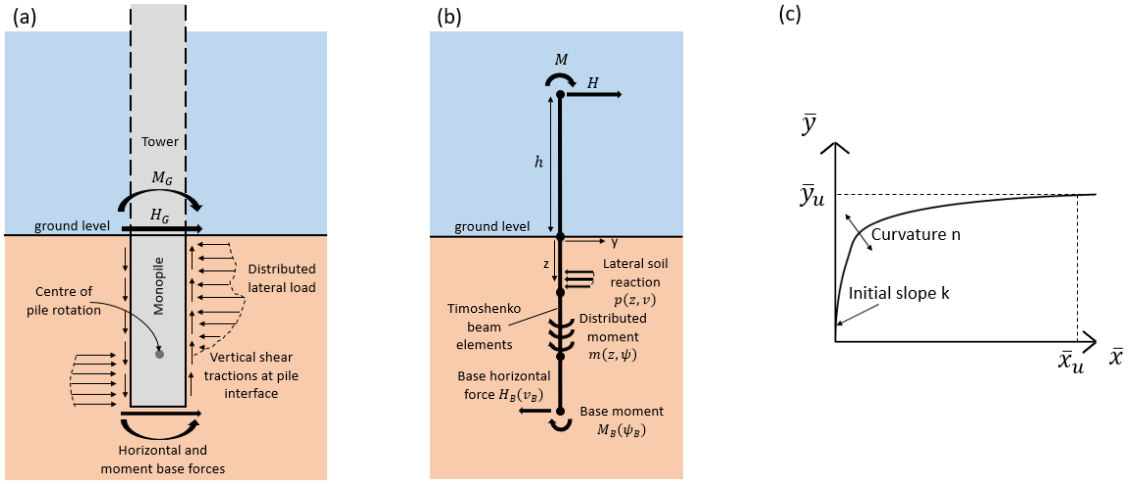

Figure 1. PISA design model. (a) Soil reaction components acting on the pile. (b) 1D finite element model framework of the embedded monopile, (c) four-parameter conic function used to represent the PISA soil reaction curves.

The PISA design model is implemented in the 1D finite element framework illustrated in Figure 1(b). A line mesh of beam elements – employing Timoshenko theory – is employed for the pile. The soil is represented by a separate set of line soil elements. Each embedded pile element is associated with a soil element attached to its two nodes. Soil-structure interaction is modelled via the soil elements using non-linear formulations employing the Winkler assumption (i.e. each soil reaction component is related only to the corresponding local lateral displacement or rotation).

To conduct analyses using the PISA design model, a monotonic lateral load H, corresponding to environmental loading, is applied at a load eccentricity h above the ground level. This is equivalent to a lateral load ($H_G = H$) and a moment load ($M_G = hH$) applied at ground level. Vertical loads applied to the monopile are neglected. The soil reaction components used in the PISA design model are calibrated by three-dimensional (3D) finite element (FE) analyses employing advanced soil constitutive models. A four-parameter conic function – relating normalized forms of pile displacement/rotation and local force/moment – is used to represent each soil reaction curve (Figure 1 (c)). Simple functions are employed to represent the depth variation along the pile of the 4-conic function parameters for each soil reaction component.

2 PICASO data-driven design method

The data-driven design method (Suryasentana et al., 2020) developed during the PICASO project employs the basic framework of the PISA design model but with Gaussian process regression (GPR) machine learning (ML) models used to formulate the soil reaction curve data. This is a form of supervised learning, where a set of training examples is available that consists of inputs (soil profile properties, pile geometries) and outputs (soil reaction curves parameters), with the aim of producing a function that maps the inputs to the outputs. The data-driven design method is an alternative to the PISA conic function-based design procedure described above; it facilitates a high-fidelity representation of the soil reaction curves – as computed with 3D finite element calibration calculations – than is possible with the original PISA design model.

2.1 *Machine learning model approach*

Gaussian process regression (GPR) is a machine learning model that assumes a Gaussian probability distribution over a range of possible random functions (Rasmussen and Williams, 2006). The procedure provides a built-in variance measure which quantifies the prediction uncertainty. GPR is a non-parametric model meaning that its expressiveness increases with the amount of data. A GPR model is fully characterized by its mean function $m(x)$ and its covariance function (kernel) $k(x, x')$ (Equation (1)), where (x, x') are inputs in either the training or the test sets. The kernel function specifies the similarity between the inputs based on the assumption that if the (x, x') inputs are similar then the $y(x)$, $y(x')$ predicted outputs will be strongly correlated.

$$f(x) \sim GP(m(x), k(x, x')) \quad (1)$$

In this paper a zero-mean function $m(x) = 0$ is adopted; this is adequate to capture the complexity of the data. A Matérn kernel (Rasmussen and Williams, 2006) with $\nu = 5/2$ is selected as a kernel function (Equation (2)).

$$k_{Matern}(r) = \frac{2^{1-\nu}}{\Gamma(\nu)} \left(\frac{\sqrt{2\nu} r}{l}\right)^{\nu} K_{\nu} \left(\frac{\sqrt{2\nu} r}{l}\right) \quad (2)$$

where Γ is the gamma function, K_{ν} is the modified Bessel function of the second kind and ν, r are positive parameters of the covariance. The Matérn kernel is a generalisation of the squared exponential kernel, which has an additional parameter ν that controls the smoothness of the function.

2.2 *Soil reaction curves formulation*

Each soil reaction curve is defined by eight 'knot point' values of soil reaction forces/moments at predefined values of the local pile displacement/rotation. The values of the force/moment at each knot point are considered as 'soil reaction curves parameters'; these data are used to train GPR models. The Piecewise Cubic Hermite Interpolating Polynomial (PCHIP) (Fritsch and Carlson, 1980) is used to interpolate the soil reaction curves from the knot points predicted by the GPR models. An example of an eight knot point piecewise soil reaction curve employing PCHIP interpolation, for normalised displacement, $\bar{v}$, and lateral soil reaction, $\bar{p}$ is shown in Figure 2.

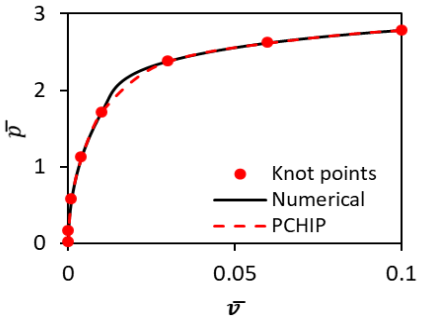

Figure 2. Example eight knot point soil reaction curve for distributed lateral load (where $\bar{p}$ is normalised lateral load and $\bar{v}$ is normalised lateral displacement). The black line indicates data extracted from a calibration 3D FEA; the red markers show the knot points; the red dotted line is the PCHIP interpolation.

3 General Cowden clay model

The general Cowden clay model (GCCM) is generated using the data-driven design method described above. The GCCM provides depth variation predictions of the knot points for each of the soil reaction curves. PCHIP interpolation is employed to generate continuous soil reaction curves which are then employed within the 1D design model illustrated in Figure 1(b). The soil reaction curves used to calibrate the model in the current work were generated using 3D FE analysis employing the PLAXIS software (Brinkgreve et al., 2018). Procedures to develop the GCCM (generation of idealised offshore clay till soil profiles, numerical modelling, soil reaction curves processing and GPR training) are outlined below.

3.1 *Generation of idealised offshore clay till soil profiles*

The glacial till clays occurring in the North Sea are typically overconsolidated due to previous glaciation periods. Consistent with previous approaches (e.g. Boulton and Dobbie, 1993) it is assumed that overconsolidation was caused solely by the prior action of the weight of ice. To define the stress history of the soil, one-dimensional compression theory is employed. This approach does not account for possible stress history effects relating to geological processes such as erosion and deposition or the influence of shear stresses applied to the soil by glacier movements. On this basis the overconsolidation ratio, OCR, at a particular soil depth is determined as the ratio between the preconsolidation stress (σ'_c) and the current vertical effective stress (σ'_v) at that depth ($OCR = \sigma'_c/\sigma'_v$). The preconsolidation stress is estimated by applying an overburden pressure – corresponding to the weight of an assumed thickness of ice sheet – to the current soil surface. A similar approach was employed in Le et al. (2014) to estimate the OCR profile of the Bolders bank glacial tills located at the Hornsea offshore wind farm. The OCR profile at a depth z below the seabed is therefore defined as follows:

$$OCR = \frac{\sigma'_c}{\sigma'_v} = \frac{\gamma_{ice} \times d_{ice} + \gamma' \times z}{\gamma' \times z} \quad (3)$$

where $\gamma' = 11.38\ \mathrm{kN/m^3}$ (Zdravkovic et al., 2020a) is the effective unit weight of Cowden till $\gamma_{ice} = 9\ \mathrm{kN/m^3}$ is adopted for the unit weight of an ice sheet with assumed thickness d_{ice}. It is assumed that the soil is submerged (non-frozen pore water) during the assumed idealized geological process.

The coefficient of lateral earth pressure (K_o) is estimated by Mayne and Kulhawy (1982),

$$\mathrm{K_{0OC}} = \mathrm{K_{0NC}} \times \mathrm{OCR}^{\sin\phi'_{cs}} \quad (4)$$

where K_{0NC} is an assumed value of K_o defined by $K_{0NC} = 1 - \sin\phi'_{cs}$; based on triaxial compression data in Zdravkovic et al. (2020a), the critical state friction angle is assumed to be $\phi'_{cs} = 27°$. Equation (4) predicts unrealistically high values of K_o for high-OCR marine clays at depths of 10m or less (Brosse et al., 2017). In the current work, therefore, the K_o profile is limited to a maximum value of 1.5-1.75.

The undrained shear strength profile for triaxial compression conditions is calculated by Equation (5) (Potts and Zdravkovic, 1999); this equation is based on the Modified Cam Clay framework as employed in the PISA project (Zdravkovic et al., 2020b).

$$s_u = OCR \times \sigma'_{V0} \times g(\theta) \times \cos(\theta) \times \frac{1+2K_{0NC}}{6} \times (1+B^2) \times \left[\frac{2\times(1+2K_{0OC})}{(1+2K_{0NC})\times OCR\times(1+B^2)}\right]^{\frac{\kappa}{\lambda}} \quad (5)$$

where $g(\theta)$ is a function used to obtain a Mohr-Coulomb hexagon for the yield surface in the deviatoric plane and B is a parameter depending on the values of $g(\theta)$ and K_{0NC}. For triaxial compression conditions the Lode's angle is $\theta = -30°$. The intact compressibility coefficient is $\lambda = 0.115$; and the swelling coefficient is $\kappa = 0.021$ (Zdravkovic et al., 2020a). Based on the approach adopted in the PISA project (Zdravkovic et al., 2020a), the small strain shear modulus (G_0) is assumed to be related to the mean effective stress by $G_0 = 1100p'$.

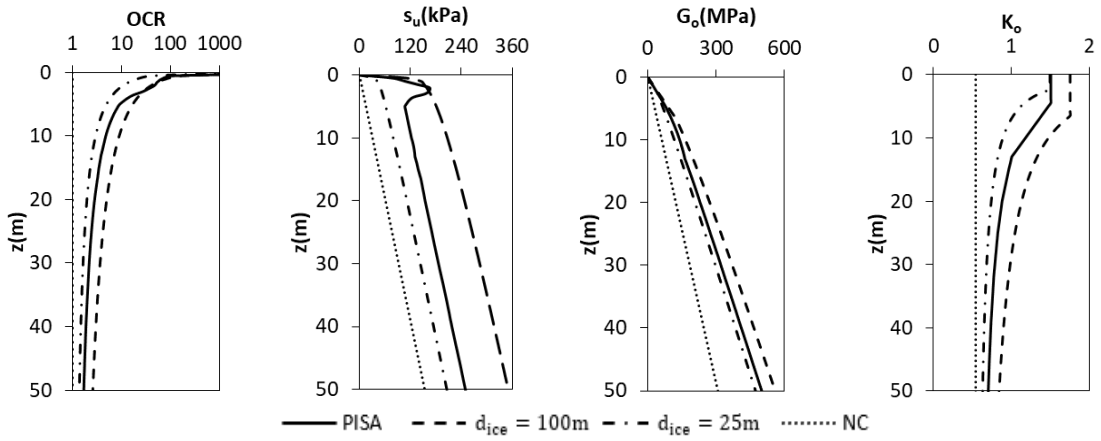

Figure 3. OCR, s_u, G_o and K_o, for the four offshore idealised offshore clay till soil profiles used to calibrate the GCCM. This set of profiles includes the representative offshore glacial clay till site employed in the PISA project (Byrne et al., 2020b).

For the current work three new idealised clay till profiles were developed as follows:

- a normally consolidated (NC) clay till profile;
- a slightly overconsolidated clay till corresponding to a previous ice sheet of thickness $d_{ice} = 25m$; and
- a heavily overconsolidated idealised clay till corresponding to a previous ice sheet of thickness $d_{ice} = 100m$.

These three idealised profiles span a range of typical clay till profiles at offshore wind farms (Le et al., 2014). It is expected that the glacial till profiles will show significant variability across a wind farm site (Clarke, 2018).

The OCR, s_u, G_o and K_o, distributions for the three idealised offshore clay till profiles are shown in Figure 3 together with the representative offshore glacial till profile adopted in the original calibration of the PISA design model (Byrne et al., 2020b). These four soil profiles represent the range of site characteristics employed in the current work to calibrate the GCCM.

3.2 *Numerical modelling*

3.2.1 *Constitutive model selection*

Calibration data were computed using PLAXIS 3D with the NGI-ADP constitutive model (Grimstad et al., 2012) to represent the clay till. NGI-ADP is a total stress model formulated for undrained analysis of clays; it is capable of capturing soil strength anisotropy by incorporating different undrained shear strength (s_u) values for different stress conditions. The model is capable of providing an approximate fit to the soil response measured in triaxial or direct shear stresses tests by means of three parameters γ_f^C, γ_f^E, γ_f^{DSS} (shear strains at failure), which define a bespoke hardening law for the yield function.

3.2.2 *Constitutive model calibration*

The γ_f^C parameter was determined by performing simulations of triaxial compression (TXC) tests in PLAXIS 3D to achieve a best fit with the PISA TXC data in Zdravkovic et al. (2020b) (see Figure 4). The parameter is determined by Minga and Burd (2019),

$$\gamma_c^f = K_f \times 100/\frac{G_{ur}}{s_u^A} \quad (6)$$

where K_f is a calibration parameter, s_u^A is the plane strain undrained shear strength ($s_u^A = s_u^{TXC}/0.99$ where s_u^{TXC} is the triaxial compression shear strength) and G_{ur} is the unloading shear modulus ($G_{ur} = G_o$). A value of $K_f = 110$ was estimated to provide the best fit to the PISA TXC tests.

The undrained shear strength for the triaxial extension conditions s_u^{TXE} was calculated by defining the model input ratio of $s_u^{\mathrm{TXE}}/s_u^A = 0.833$ (Minga and Burd, 2019). The undrained shear strength for direct simple shear s_u^{DSS} was computed by averaging the undrained shear strengths from TXC and TXE ($s_u^{DSS}/s_u^A = 0.911$) as suggested by Liu et al. (2020) for Cowden till. Since the model is being used for offshore calculations, the effective bulk unit weight is used to determine the depth profile of effective stress. The initial mobilised maximum shear stress (τ_0) is determined by τ_0/s_u^A ratio calculated from Equation 7 (Brinkgreve et al., 2018); a value of zero is adopted if the calculated ratio is negative.

$$\tau_0/s_u^A = 0.5(1 - K_0) \times \sigma'_{v0}/s_u^A \quad (7)$$

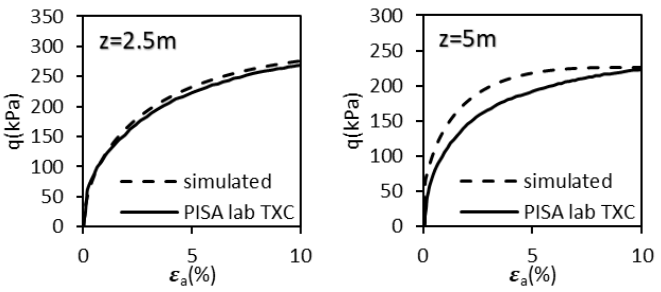

Figure 4. Simulation of undrained TXC tests in PLAXIS 3D with PISA laboratory TXC tests (Zdravkovic et al., 2020b) $q - e_a$ response for soil samples retrieved at 2.5m, 5m.

3.2.3 *3D analysis model geometry*

The mesh adopted in the PLAXIS 3D calibration analyses incorporates a plane of symmetry; only half of the problem is simulated. The bottom boundary was set at a depth of 100m; the other mesh dimensions were $12D$, in the X direction and $4D$ in the Y direction, where D is the monopile diameter (Figure 6(c)). A fixed constraint was used for the bottom boundary of the model. The side boundaries and the plane of symmetry were fixed in the normal direction only. The meshes comprised between 90000 and 110000 10-noded tetrahedral elements. The load applied at the top of the pile is simulated by applying a prescribed displacement u_x in the X direction at the required load eccentricity height h.

The pile was modelled using plate elements. The steel pile material is assumed to be linear elastic with a Young's modulus $E = 200\text{GPa}$ and Poisson's ratio $\nu = 0.30$. The pile was wished in place, hence installation effects are disregarded.

Interface elements were used around the pile to model the pile-soil interaction. The interface elements were modelled with a Mohr-Coulomb material with a 'Drained Calculation Type' in PLAXIS. The strength parameter of the interface properties was reduced by a factor of 0.65 compared to the surrounding ground. A tension cut-off criterion was adopted to model possible gap formation behind the pile. A value of 10^5kN/m^3 was adopted for the elastic normal (K_N) and shear stiffness (K_s) of the interface elements (Zdravkovic et al., 2020b).

The total number of sublayers generated in PLAXIS 3D was carefully selected for each soil profile to allow the required G_o and s_u profiles to be accurately simulated (Figure 5). The NGI-ADP model in PLAXIS 3D adopts, for each sublayer, a linear depth variation of s_u and G_o, and a constant value of K_o . The simulated G_o profile is calculated using the specified G_{ur}/s_u^A ratio. In the PLAXIS NGI-ADP implementation, the G_{ur}/s_u^A ratio is limited to a maximum of 2000; this limit causes a slight underprediction of the required G_o profile at the bottom sub-layers of the soil profiles, as illustrated in Figure 5.

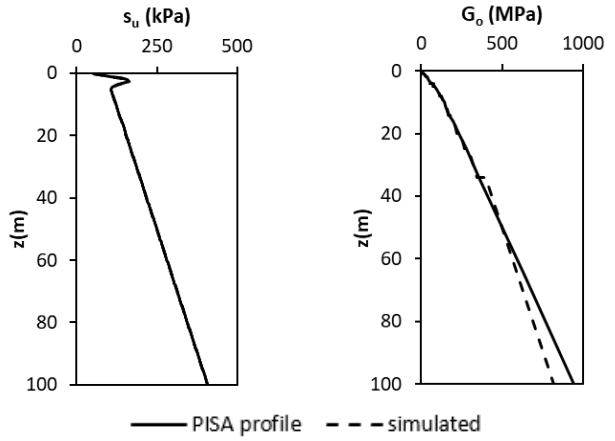

Figure 5. Simulated s_u, G_o profiles represented by the NGI-ADP model compared to the PISA representative offshore glacial clay till profile (Byrne et al., 2020b).

3.2.4 *Pile geometry calibration space*

The pile geometry calibration space adopted for each soil profile is specified in Table 1; this employs nine of the eleven calibration pile geometries adopted in Byrne et al. (2020b), to develop the PISA 1D Cowden till model. The calibration piles adopt geometries that are representative of typical offshore pile configurations with values of *L/D* between 2 and 6. The normalised load eccentricity, *h/D*, is 5 for wave-dominated loading and 15 for wind-dominated loading.

Table 1. Pile geometry calibration space. L is the embedded length; D is the pile diameter; h is the load eccentricity; t is the pile wall thickness

Pile	D(m)	L(m)	t(mm)	h(m)
C1	10	20	91	50
C2	10	20	91	150
C3	10	60	91	50
C4	10	60	91	150
C5	5	10	45	25
C6	5	30	45	25
C7	5	30	45	75
C8	7.5	15	68	37.5
C9	7.5	45	68	37.5

3.2.5 *Validation of finite element modelling*

To assess the performance of the NGI ADP model, analyses were conducted to compare with the finite element analyses – based on an extended modified Cam Clay effective stress model - described in Byrne et al. (2020b). These analyses are concerned with the representative offshore glacial clay till site specified in Byrne et al. (2020b). A comparison between two sets of calculations; 'ultimate response' (ground level pile displacement v_G up to $v_G = D/10$) and 'small displacement response' (ground level pile displacements up to $v_G = D/10000$) is shown in Figure 6. The current NGI ADP results compare well with the data in Byrne et al. (2020b).

3.3 *Soil reaction curves extraction and data-processing*

Soil reaction curves were extracted from each of the 36 calibration FEA as follows. Data were obtained on the computed traction forces at the interface element Gauss points and the displacements at the plate element nodes. This information was used to determine sets of numerical soil reaction curves for the four soil reaction components illustrated in Figure 1b. The forces/moments (p, m, H_b, M_b) were normalised using the PISA framework described in Byrne et al (2020b). A different normalisation procedure was adopted for the displacement/rotation variables; the adopted normalised displacement is $\bar{v} = v/D$ and the normalised rotation is $\bar{\psi} = \psi$. The eight knot point forces at predefined values of normalised pile displacement/rotation were determined for each soil reaction component to train the GPR model.

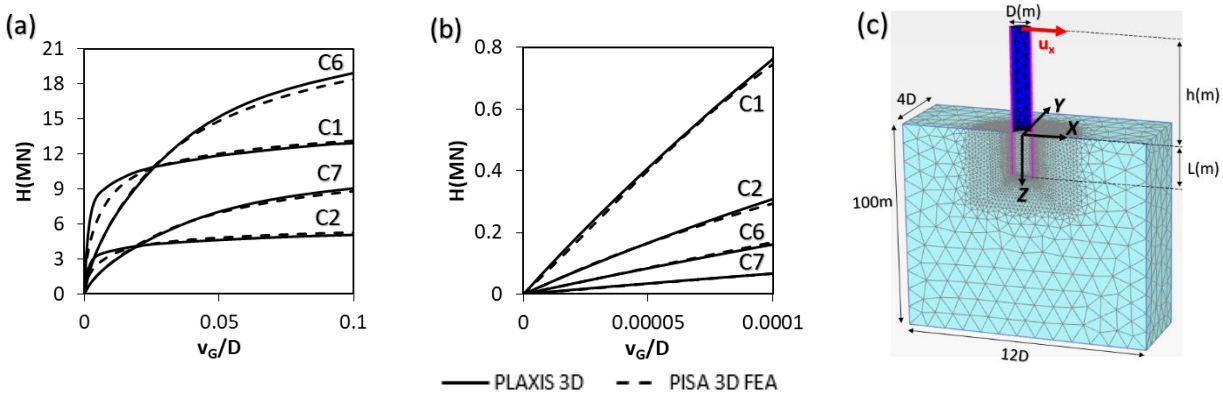

Figure 6. Load-displacement responses at ground level for four of the calibration piles embedded in the PISA representative offshore glacial clay till site computed by the 3D FE model in Byrne et al., (2020b) and the current NGI-ADP PLAXIS 3D results for: (a) ultimate response, (b) small displacement response. Figure(c) shows an example FE mesh (for pile C1) employed in the current work.

3.4 *GPR model training*

3.4.1 *Inputs*

The GPR model employs four inputs; (L/D) is a proxy for the pile slenderness; (z/L) allows the depth variation of the knot points to be captured; (G_o/s_u) discriminates locally the soil reaction curves with the same values of (z/L) and (L/D); (s_u/σ'_v) (where σ'_v is the local vertical effective stress) is employed to discriminate between clays with different OCR profiles.

3.4.2 *Training procedure*

The normalised eight knot point soil reaction curve data are log-transformed to ensure that all prediction values are positive and physically realistic. A GPR model is trained for each of the eight knot points for each soil reaction component. The Matérn 5/2 covariance function with Automatic Relevance Determination (ARD) is employed where the σ_f^2 and l_i hyperparameters are optimised by maximising the log marginal likelihood. The White Noise kernel $k_{WN}(x, x')$ is added to the Matern kernel to account for possible noise in the dataset. An 80:20 training-test set split ratio was adopted. An approximate computational time of 20 minutes was needed for the GCCM training procedure.

3.4.3 *GPR model predictions*

The predictions – with the soil profile and pile geometry as inputs - provide:

- the depth variation for each of the eight knot point load/moment data at the predefined normalised displacements for the normalised distributed lateral load $(\bar{p})$ and normalised distributed moment $(\bar{m})$;
- predictions for each of the eight knot point force/moment data at the predefined normalised displacements/rotations for the base horizontal force $(\bar{H}_b)$ and base moment $(\bar{M}_b)$.

Figure 7 presents depth variation predictions for the ultimate force (8th knot point) for the $(\bar{p}, \bar{m})$ soil reaction components determined from the trained GPR model. These predictions relate to calibration pile C1 and the PISA idealised offshore clay till soil profile. The Matern kernel function that is employed can accurately predict the complex depth variation of this particular distributed lateral and moment reaction data along the monopile. The GPR model also provides the 95% confidence interval. In this example the uncertainty is small since the results are predicted for a trained pile geometry/soil profile combination. The estimation of the prediction's uncertainty is a key advantage of the data-driven approach since the GPR model can quantify the uncertainty in cases of unseen pile geometries or soil profiles.

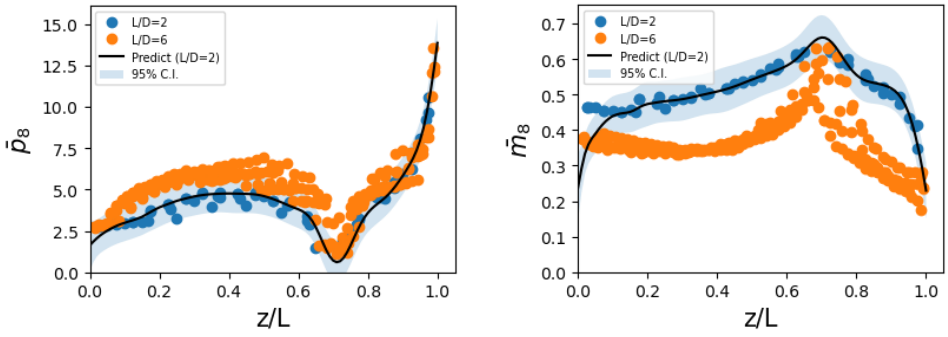

Figure 7. Example GCCM outputs for the 8th knot point for distributed load and moment for the C1 pile $(L/D = 2)$ and the PISA representative offshore glacial clay till profile: The depth variation of the mean GPR prediction for $\bar{p}_8$, $\bar{m}_8$ knot points is indicated by the black line. The 95% confidence interval is shown (shaded bounds). The i) orange markers, ii) blue markers are the trained data-points from i) $L/D = 6$ and ii) $L/D = 2$ piles.

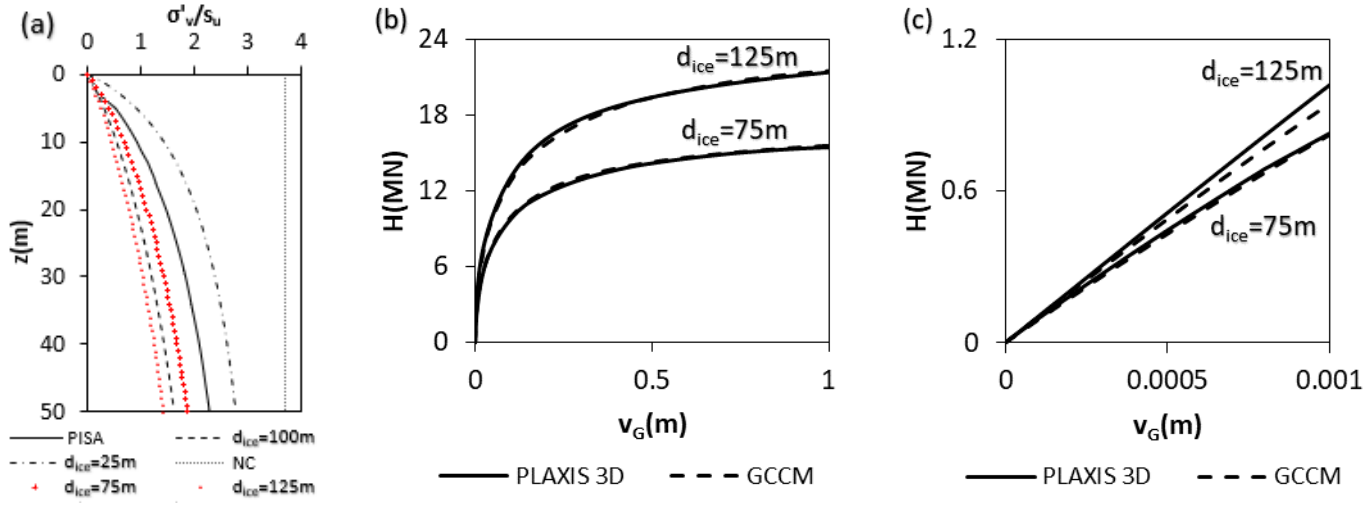

Figure 8. (a) Variation with depth of (σ'_v/s_u) for two unseen clay till profiles with OCR profiles generated with $d_{ice} = 75$ m and $d_{ice} = 125$ m (indicated by the red markers) compared with the four idealised profiles used to calibrate the GCCM, (b) Pile load-displacement response predicted by the GCCM for the ultimate response compared with PLAXIS 3D results, (c) Pile load-displacement response predicted by the GCCM for the small displacement response compared with PLAXIS 3D results.

4 Design examples

To demonstrate the predictive capability of the GCCM, three design examples are presented. These examples are concerned with:

- monopile geometries within the calibration space embedded in unseen clay soil profiles; and
- PISA field test monopile, outside the calibration space.

Two unseen idealised offshore clay soil profiles were introduced corresponding to the previous ice sheets with thickness $d_{ice} = 75$ m and $d_{ice} = 125$ m. The (σ'_v/s_u) depth profiles for these unseen cases are compared with the calibration profiles in Figure 8 (a); one of the unseen cases falls inside the range of calibration soil profiles and the other falls outside. Figures 8(b), 8(c) show the load-displacement ultimate and small displacement responses for pile C1 (Table 1) computed using the 1D model employing the GCCM; corresponding PLAXIS 3D analyses are also shown. The GCCM provides a close representation of the more detailed 3D finite element calculation for both of the unseen soil profiles.

The CM9 PISA Cowden field test pile (Byrne et al., 2020a), employing the strength and stiffness profiles for the Cowden test site (Zdravkovic et al. 2020a, b) is selected to demonstrate the predictive capability of the GCCM for a pile geometry outside of the calibration space. The CM9 pile has a length $L = 3.98$m, a diameter $D = 0.762$m, load eccentricity $h = 9.98$m and wall thickness $t = 11$mm. This pile geometry has a (L/D) value within the trained calibration space but the diameter is smaller than the trained pile diameters. Figure 9 presents the load-displacement response at ground level computed using the GCCM for this case. The result is compared to the PLAXIS 3D prediction, the measured field test response in Byrne et al. (2020a) and the computed result using the PISA 1D Cowden till model described in Byrne et al., (2020b). The GCCM provides an accurate representation of the field data. The relatively poor performance of the PISA Cowden 1D model is unsurprising as the model is being used here outside of its calibration space.

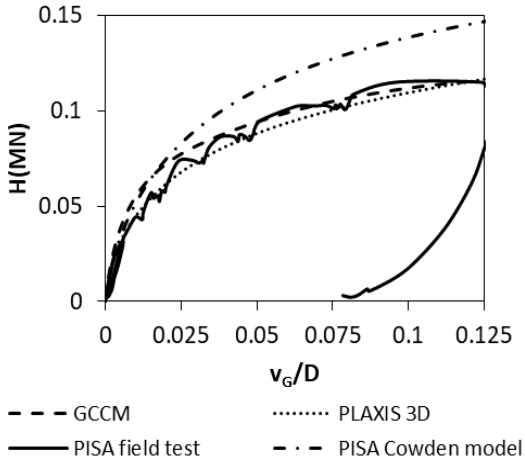

Figure 9. Pile load-displacement response computed with the GCCM for the CM9 PISA field test pile compared with the PLAXIS 3D results, the PISA field test data and predictions using the original PISA design model for Cowden till (Byrne et al., 2020a)

5 Conclusions

A general glacial clay till 1D model was generated for monotonic laterally loaded monopiles embedded in homogenous clay till soil with various OCR profiles. Soil characteristics employed in the model are based on data from the PISA Cowden test site. This data-driven method is suitable for generating general unified clay models for offshore clay soil sites with different stress histories by incorporating (s_u/σ'_v) - which is closely related to the OCR – as an input

feature. The built-in variance measure of the GPR ML model can estimate the uncertainty of the predictions. The GCCM can accurately predict the monotonic lateral load behaviour of monopiles with L/D values ranging from 2 to 6 for soil profiles with (s_u/σ'_v) falling inside the trained calibration space. It was demonstrated that the model can also provide reliable predictions for soil profiles falling marginally outside of the trained (s_u/σ'_v) calibration space. Furthermore, the model is shown to accurately capture the response of one of the PISA field test monopiles; this demonstrates the capability of the model to capture the response of piles with a diameter that is smaller than the piles in the training set (although with (L/D) that falls within the calibration space. The approach presented in the paper is readily extended to account for different types of clay soil profiles.

6 Acknowledgements

The authors acknowledge the support of Ørsted for supporting the PICASO project. Byrne is supported by the Royal Academy of Engineering under the Research Chairs and Senior Research Fellowships scheme.

7 References

Boulton, G. and Dobbie, K. (1993). 'Consolidation of sediments by glaciers: Relations between sediment geotechnics, soft-bed glacier dynamics and subglacial ground-water flow'. Journal of Glaciology, 39(131), 26-44. doi:10.3189/S0022143000015690.

Brinkgreve, R.B.J., Kumarswamy, S. and Swolfs, W.M. (2018). Plaxis manual 2018. Plaxis bv Delft, the Netherlands.

Brosse, A., Kamal, R. H., Jardine, R. J. and Coop, M. R. (2017). 'The shear stiffness characteristics of four Eocene- to-Jurassic UK stiff clays'. Géotechnique, 67 (3), pp. 242–259.

Burd, H.J., Taborda, D.M.G., Zdravkovic, L., Abadie, C.N., Byrne, B.W., Houlsby, G.T., Gavin, K.G., Igoe, D.J.P., Jardine, R.J., Martin, C.M., McAdam, R. A., Pedro, A.M.G. and Potts, D. (2020a). 'PISA design model for monopiles for offshore wind turbines: application to a marine sand'. Géotechnique 70, No. 11, 1048–1066.

Byrne, B. W., McAdam, R. A., Burd, H. J., Houlsby, G. T., Martin, C. M., Beuckelaers, W. J. A. P., Zdravkovic´, L., Taborda, D. M. G., Potts, D. M., Jardine, R., Ushev, E., Liu, T., Abadias, D., Gavin, K., Igoe, D., Doherty, P., Skov Gretlund, J., Pacheco Andrade, M., Muir Wood, A., Schroeder, F. C., Turner, S. & Plummer, M. A. L. (2017). PISA:new design methods for offshore wind turbine monopiles. In Proceedings of the 8th international conference on offshore site Investigation and geotechnics, smarter solutions for offshore developments, vol. 1, pp. 142–161. London, UK: Society for Underwater Technology.

Byrne, B. W., McAdam, R. A., Burd, H.J., Beuckelaers, W. J. A., Gavin, K. G., Houlsby, G.T., Igoe, D. J. P., Jardine, R. J., Martin, C.M., Wood, A. M., Potts, D. M., Gretlund, J. S., Taborda, D. M. G., and Zdravković L. (2020a). 'Monotonic laterally loaded pile testing in a stiff glacial clay till at Cowden'. Géotechnique 70, No. 11, 970–985.

Byrne, B. W., Houlsby, G. T., Burd, H. J., Gavin, K. G., Igoe, D. J. P., Jardine, R. J., Martin, C. M., McAdam, R. A., Potts, D. M., Taborda, D. M. G. and Zdravkovic, L. (2020b). 'PISA design model for monopiles for offshore wind turbines: Application to a stiff glacial clay till'. Géotechnique 70, No. 11, 1030–1047.

Clarke, B. G. (2018). The engineering properties of glacial tills. Geotechnical Research, 5(4), 262-277.

DNVGL. (2016). DNVGL-ST-0126 – Support structure for wind turbines. Oslo: Det Norske Veritas.

Grimstad G., Andersen L., Jostad H. P. (2012). 'NGI-ADP: Anisotropic shear strength model for clay'. International Journal for Numerical and Analytical Methods in Geomechanics. 36(4):483 – 497. DOI: 10.1002/nag.1016.

Fritsch, F.N. and Carlson, R.E. (1980). 'Monotone Piecewise Cubic Interpolation, SIAM'. Journal on Numerical Analysis, 17, pp. 238-246.

Le, T. M. H., Eiksund, G. R., Strøm, P. J., & Saue, M. (2014). 'Geological and geotechnical characterisation for offshore wind turbine foundations: A case study of the Sheringham Shoal wind farm'. Engineering geology, 177, 40-53.

Liu, T., Ushev, E. R., & Jardine, R. J. (2020). 'Anisotropic stiffness and shear strength characteristics of a stiff glacial till'. Journal of Geotechnical and Geoenvironmental Engineering, 146(12).

Mayne, P. W., and Kulhawy, F. H. (1982). 'Ko-OCR relationships in soil'. Journal of the Geotechnical Engineering Division, 108(6), 851-872.

Minga, E. and Burd, H.J. (2019a). Validation of PLAXIS MoDeTo based on the Cowden Till PISA Field Tests, Oxford University: Oxford, UK.

Potts, D. M. and Zdravković, L. T. (1999). Finite element analysis in geotechnical engineering: Theory, London: Thomas Telford.

Rasmussen, C. E. and Williams, C. K. I. (2006). Gaussian Processes for Machine Learning. MIT Press.

Suryasentana, S. K., Burd, H. J., Byrne, B. W, Aghakouchak, A. and Sørensen, T. (2020b). 'Comparison of machine learning models in a data-driven approach for scalable and adaptive design of laterally-loaded monopile foundations'. ISFOG. Texas.

Zdravkovic, L., Jardine, R. J., Taborda, D. M. G., Abadias, D., Burd, H. J., Byrne, B. W., Gavin, K. G., Houlsby, G. T., Igoe, D. J. P., Liu, T., Martin, C. M., McAdam, R. A., Muir Wood, A., Potts, D. M., Skov Gretlund, J. and Ushev, E. (2020a). 'Ground charaterisation for PISA pile testing and analysis'. Géotechnique 70, No.11, 999–1013.

Zdravković, L., Taborda, D. M. G., Potts, D. M., Abadias, D., Burd, H. J., Byrne, B. W., Gavin, K., Houlsby, G. T., Jardine, R. J., Martin, C. M., McAdam, R. A. and Ushev, E. (2020b). 'Finite element modelling of laterally loaded piles in a stiff glacial clay till at Cowden'. Géotechnique 70, No. 11, 945–960.